

Physical Characterization of Cadmium Sulfide Thin Films Doped with Lithium Deposited Using Spray Pyrolysis Technique

Hamsa Abdul Kareem Hmoud

hamsaaljaber@yahoo.com

Ministry of Education/ General Directorate of Education in Baghdad Governorate/ Rusafa Third.

Abstract

The Spray Pyrolysis Technique was utilized to create thin films of both CdS and CdS:Li, with subsequent analysis of their structural, morphological, and optical attributes through X-ray diffraction (XRD), atomic force microscopy (AFM), and UV-visible spectroscopy, respectively. As the proportion of lithium (Li) was increased, there was an observable enlargement in grain size, transitioning from 10.11 nm to 11.07 nm. In parallel, the dislocation density exhibited a decline from 96.83 to 81.58, coupled with a reduction in strain from 34.27 to 31.31. The XRD analysis disclosed a polycrystalline structure with a pronounced alignment along the (111) plane. AFM imaging showcased a spectrum of particle dimensions within the films, ranging from 87.2 nm to 33.14 nm, with higher lithium doping levels of 1% Vol to 3% Vol. Correspondingly, the mean surface roughness (Ra) values experienced a descent from 8.85 nm to 4.34 nm, along with root mean square (RMS) values diminishing from 9.81 nm to 5.55 nm due to the lithium doping.

In the visible spectrum, all the films exhibited elevated levels of transmittance (>85%). Furthermore, as lithium doping intensified, there was a decline in the energy gap of the films, shifting from 2.40 eV to 2.09 eV. Notably, the introduction of lithium doping augmented the optical parameters, as evidenced by the elevation of these values.

Keywords: Cadmium Sulfide, lithium, Spray Pyrolysis Technique, structural, topography, and optical properties, energy gap.

Introduction

Nanostructured semiconductors have garnered significant interest in both fundamental research and cutting-edge technological applications [1]. Among these materials, CdS holds a prominent position due to its versatile applications in various advanced technologies. Furthermore, these thin films find applications in various fields such as solar cells, photochemical catalysis, nonlinear optical materials, gas detectors, luminescent devices, and optoelectronic devices [2-4]. Being a direct bandgap binary semiconductor, CdS is particularly well-suited for solar applications [5]. In the realm of solar cells, CdS is considered a favorable substitute for several heterojunction solar cells, thanks to its slightly wider energy bandgap of 2.42 eV [6]. Through the integration of CdS with substances like copper indium gallium diselenide/sulphide (CIGS), CdTe, and CuInSe₂/sulphide, the possibility arises to fabricate high-efficiency heterojunction solar cells [7]. Doping impurity substances such as boron, gallium, indium, and aluminum can enhance the properties of CdS in both optical and electrical [8-11]. Additionally, CdSe has been doped with a variety of elements to produce high concentrations of n-type or p-type CdSe carriers, such as CdSe:Sb [12], Er³⁺ [13], indium [14], and Ni [15]. Among these additions, Li can give n-type CdS better electrical behavior. By altering the doping level during synthesis, The introduction of Li³⁺ ions in CdS allows for the control and regulation of the film's shape, particle size and chemical composition,. The substitution of dopants on cadmium sites is

reduced, and the optoelectronic properties of the CdS matrix are improved by adding cationic impurities [3]. Lithium-doped CdS thin films can be created using various techniques, including CBD, spray pyrolysis, electrodeposition, sol-gel and thermal evaporation [16-19]. In the current study, Lithium can be added to CdS films at various concentrations to change their optical, structural, and characteristic properties to assess technological applications' viability. The results of the current study show how Li doping affects the investigated research.

Experimental

The spray pyrolysis technique was employed to fabricate thin films of both undoped CdS and CdS: Li. To perform the spray pyrolysis, a glass atomizer with a 60-second output nozzle was developed in a lab. The initial solution consisted of an aqueous mixture containing 0.1 M of CdCl₂ in combination with de-ionized water and ethanol. The lithium doping was introduced at concentrations of 1% and 3%. The films were then deposited onto heated glass substrates at a temperature of 400°C. created the final spray solution. Each deposition required a total of 50 ml. spray time was 10 seconds, the distance between two successive sprays was 2.5 minutes, the base-to-sprayer distance was 28 cm, and air at a pressure of 105 Pa served as the transporter gas. Thickness was measured using the weighting method around 320 ± 20 nm. XRD obtained the structural properties. AFM were applied to get the film surface. Transmittance measurements were conducted using a dual-beam spectrophotometer.

Results and Discussions

Figure 1 shows the XRD pattern that represented the deposited films. It features three prominent peaks that are assigned to the (111), (200), (222), and (400) planes, respectively, at 28.17°, 32.70°, 47.08°, and 68.93°. The JCPDS card file number for the peak at 2 value of 28.17 is conformable to the (111) plane (21-0829).

Scherrer's formula could figure the readied thin films crystallite size (*D*) by the equation underneath, as follows [20]:

$$D = \frac{0.9\lambda}{\beta \cos\theta} \quad (1)$$

Where λ is x-ray wavelength of X-ys, θ and β are Bragg's angle and (FWHM), respectively. The information that was obtained is presented in Table 1. It has been demonstrated that the value of *D* rises from 10.11 to 11.07 nm as the lithium content increases; hence, the lithium content is appropriate for determining the crystal sizes of the material. To get an estimate of the dislocation density (δ), the following expression (2) is used [21].

$$\delta = \frac{1}{D^2} \quad (2)$$

The value of δ declines from 96.83 to 81.58 as lithium content increases.

The lattice strain (ϵ) was determined utilizing the subsequent equation [22]:

$$\varepsilon = \frac{\beta \cos \theta}{4} \quad (3)$$

The value of ε decreases from 34.27 to 31.31 as lithium content increases, and Table 1 presents the computed structural coefficients (S_c) in their respective positions. Fig. 2 list the values of against lithium content.

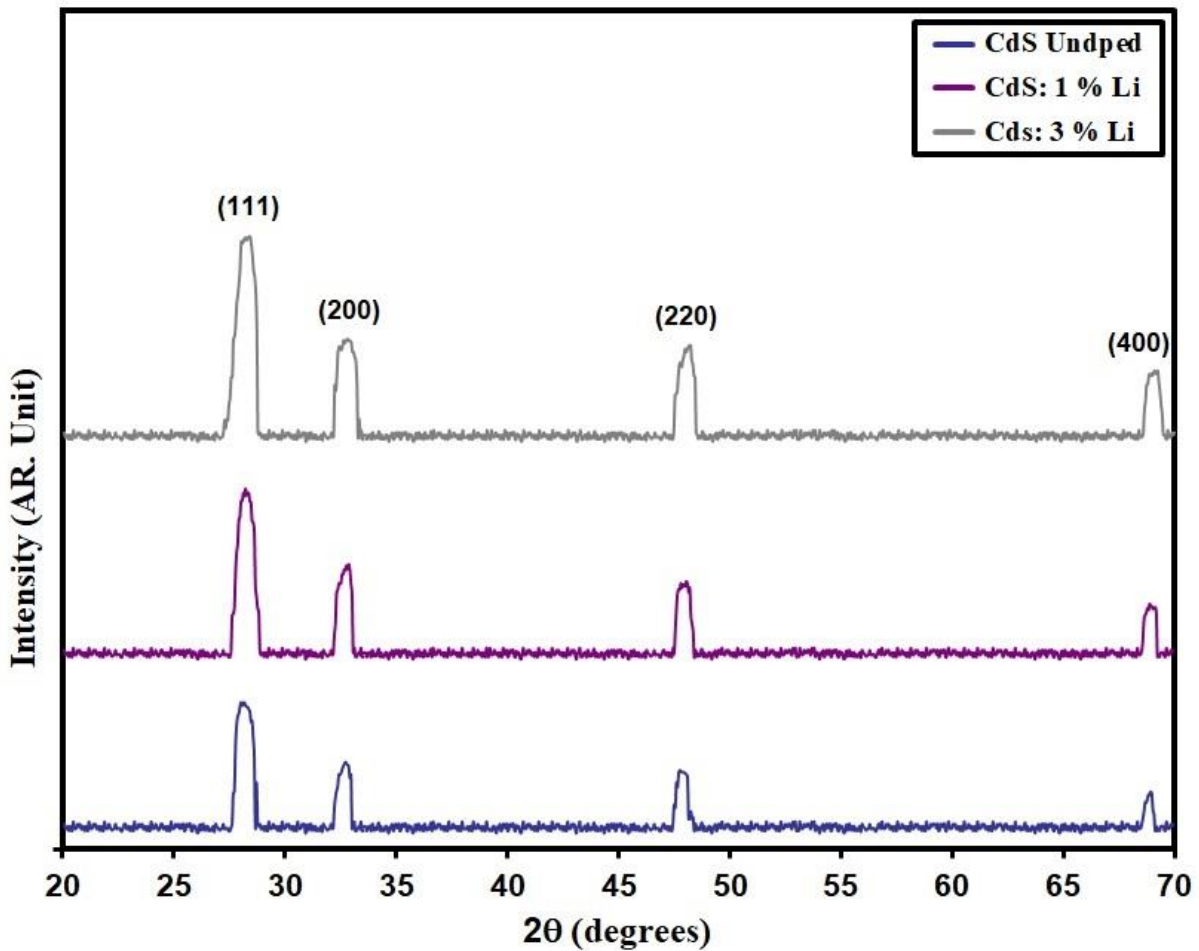


Fig.1. XRD patterns of grown films.

Table 1. D , optical bandgap and S_c of grown films.

Specimen	2θ	(hkl)	FWHM	E_g (eV)	D (nm)	δ ($\times 10^{14}$) (lines/m ²)	ε
----------	-----------	-------	------	------------	----------	---	---------------

	(°)	Plane	(°)				($\times 10^{-4}$)
Undoped CdS	28.17	111	0.81	2.40	10.11	96.83	34.27
CdS: 1% Li	28.13	111	0.77	2.34	10.63	88.83	32.58
CdS: 3% Li	28.10	111	0.74	2.29	11.07	81.58	31.31

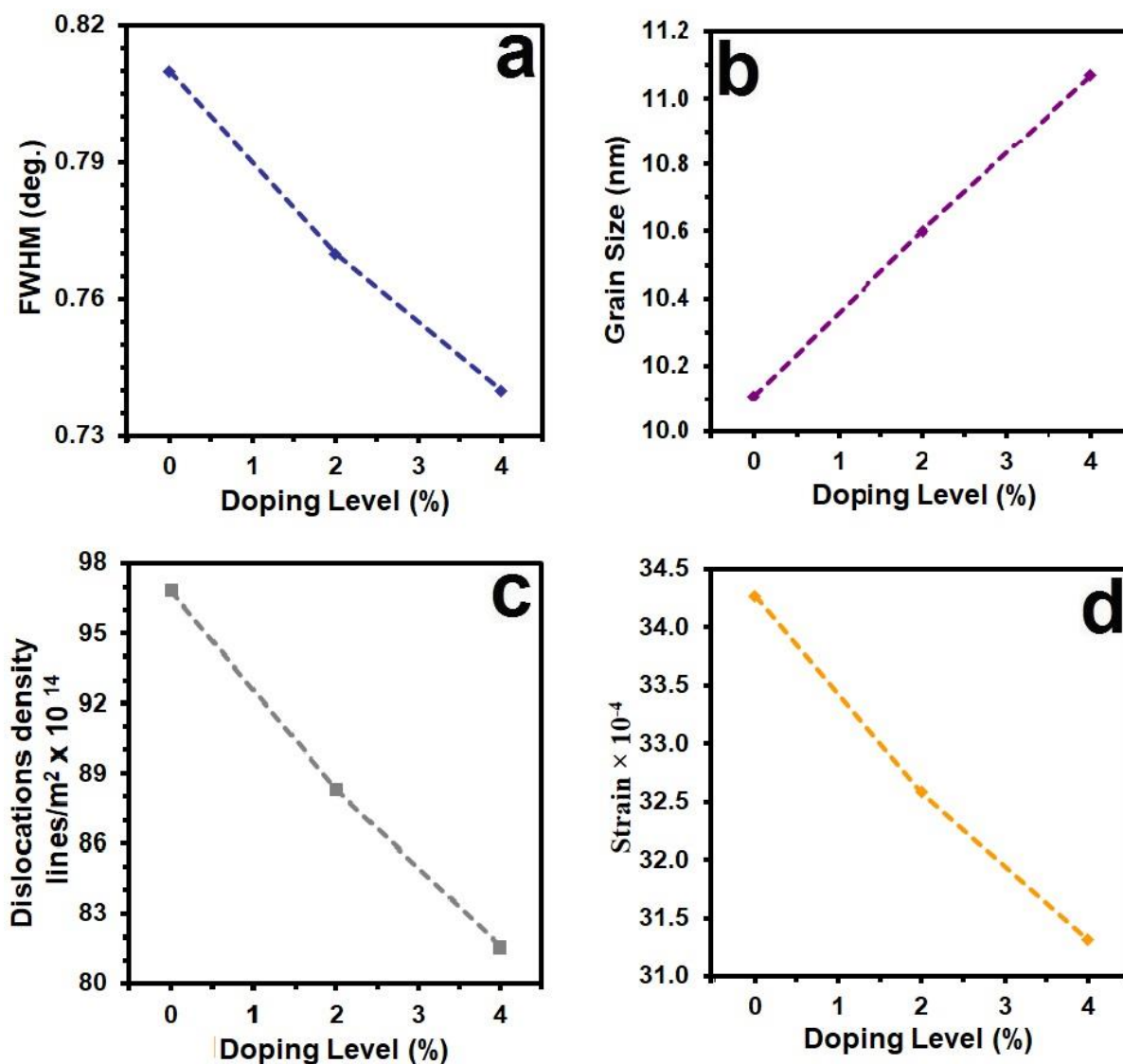


Fig.2. S_c of the intended films.

AFM pictures revealed the as-grown films' surface topography, as illustrated in Figure (3). For the (Undoped CdS, CdS:1% Li, and CdS:3% Li) films, the particle size T_p was 87.2, 75.7, and 33.1 nm, respectively. Average surface roughness R_a and RMS values decreased with

doping, falling from 8.858 to 4.34 nm and 9.81 to 5.55 nm, respectively. AFM parameters P_{AFM} against lithium dopant are given in Fig. 3 (a_3 , b_3 and c_3). Table 2 lists values of AFM parameters.

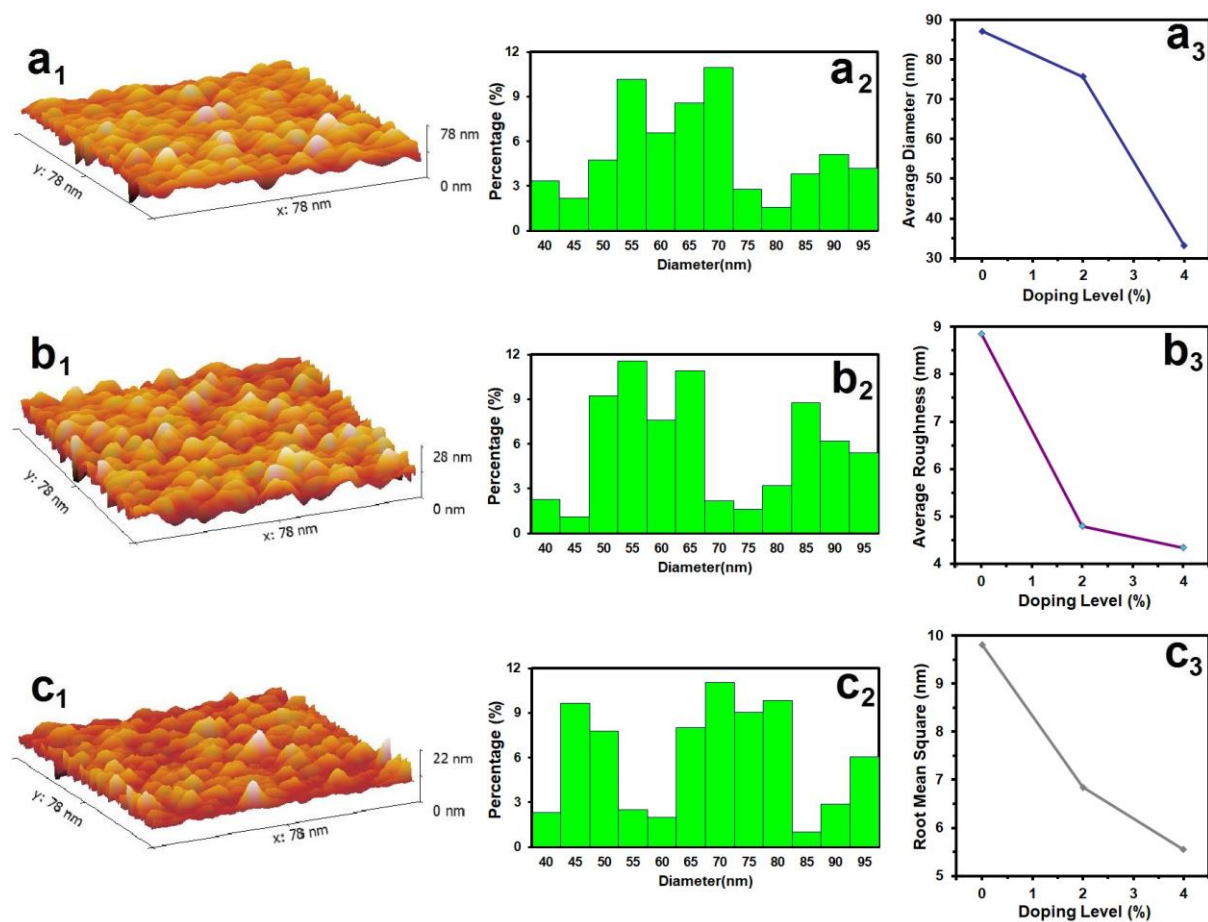


Fig.3. AFM informations of the grown films

Table 2. P_{AFM} of the intended films.

Samples	T_p nm	R_a (nm)	RMS (nm)
Undoped CdS	87.2	8.85	9.81
CdS: 1% Li	75.7	4.79	6.84
CdS: 3% Li	33.1	4.34	5.54

Figure 4 illustrates the transmittance (T) spectra of both CdS and CdS:Li thin films. Notably, transmittance levels exceeding 85% were observed across all films within the visible wavelength range. The absorption coefficient, denoted as α (λ), is characterized by the following definition [23]:

$$\alpha = (2.303 \times A)/t \quad (4)$$

Where (t) represents the thickness of the film.. Fig. (5) shows α of the intended films, and it is found that α increases with lithium content.

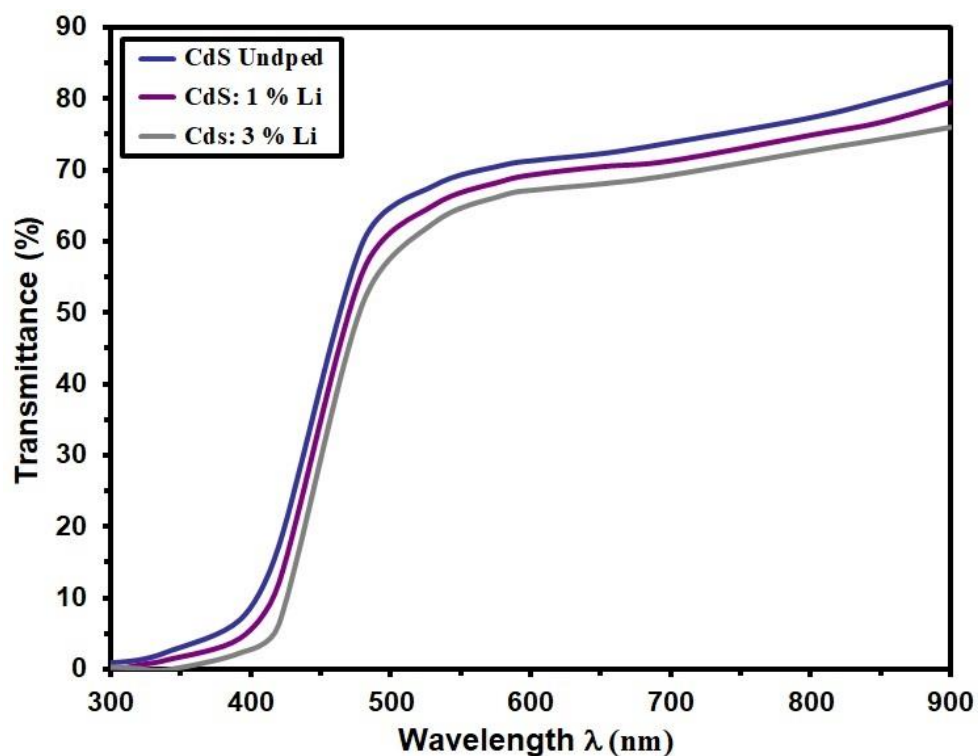


Fig. 4: Transmittance (T) as a function of wavelength for the fabricated films.

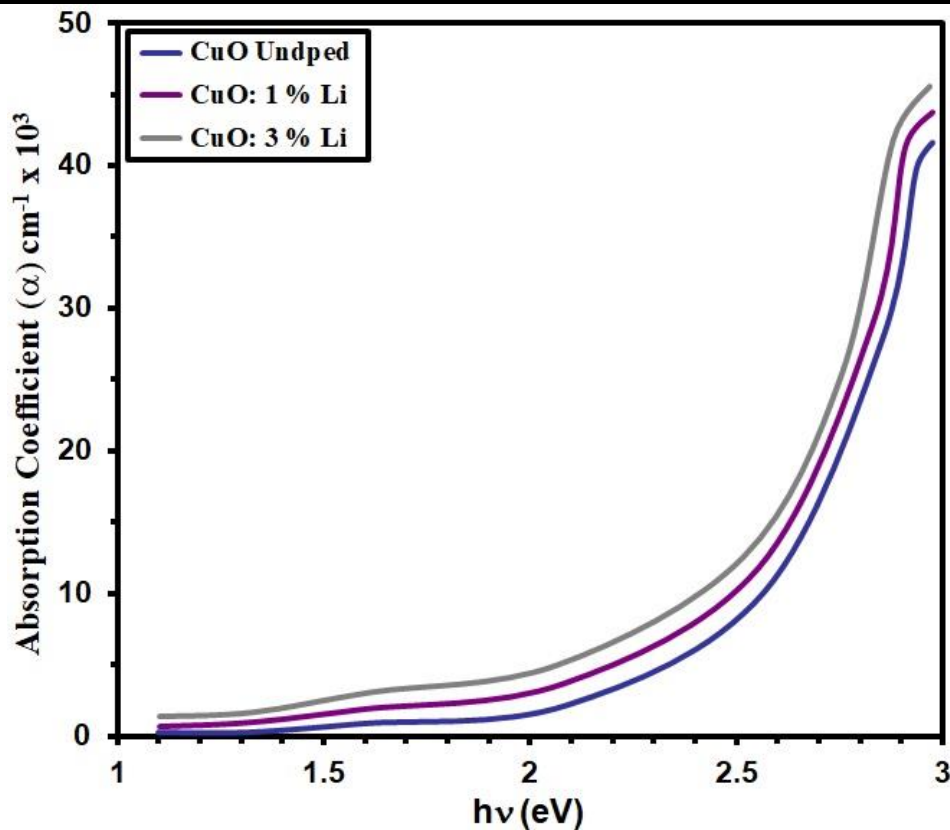


Fig. 5: absorption coefficient of the films that were prepared.

The energy gap (E_g) was calculated from the transmission data using the following equation [24]:

$$(\alpha hv) = A(hv - E_g)^{\frac{1}{2}} \quad (5)$$

where hv represents the photon energy, and A stands for absorbance. The plot of $(\alpha hv)^2$ against hv is depicted in figure (6). Notably, the values of E_g shifted from 2.40 eV to 2.29 eV with varying concentrations of lithium.

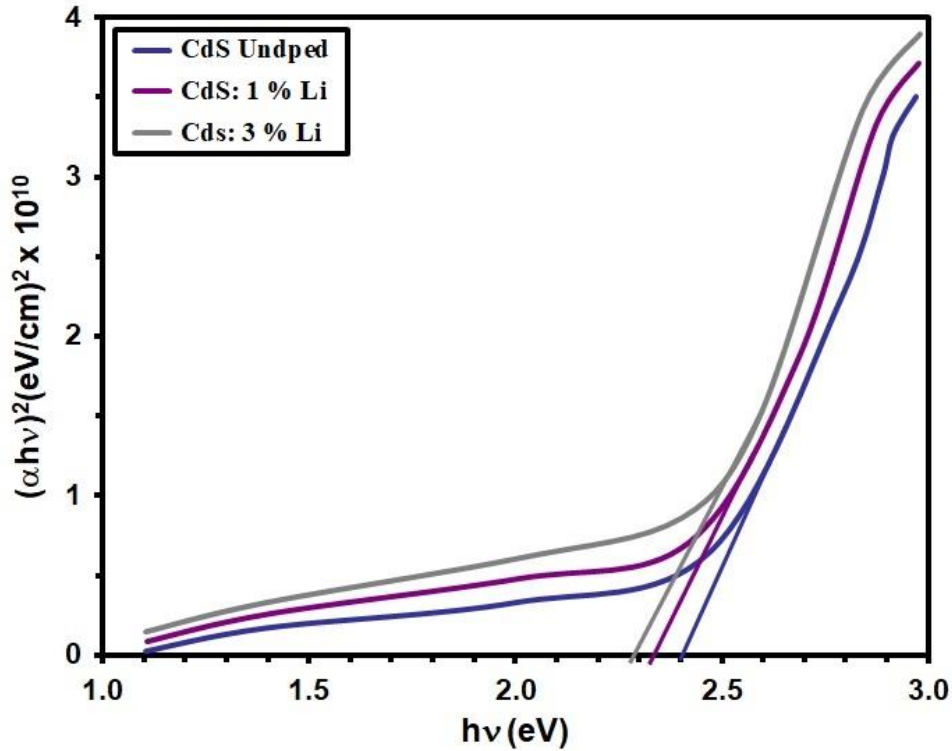


Fig. 6: E_g of CdS with different Li doping.

The extinction coefficient (k_o) can be determined using the following relationship [25]:

$$K_o = \alpha\lambda/4\pi \quad (6)$$

The plot of K_o versus λ is presented in Figure 7 for the lithium-doped CdS thin film. It's noteworthy that K_o decreases as the concentration of Li increases.

The refractive index (n) is computed based on the reflectance (R) and k using the following relationship [26]:

$$n = \left[\left(\frac{4R}{(R-1)^2} \right) - K_o^2 \right]^{1/2} - \frac{R+1}{R-1} \quad (7)$$

From Fig. 8 n declines with rising lithium content.

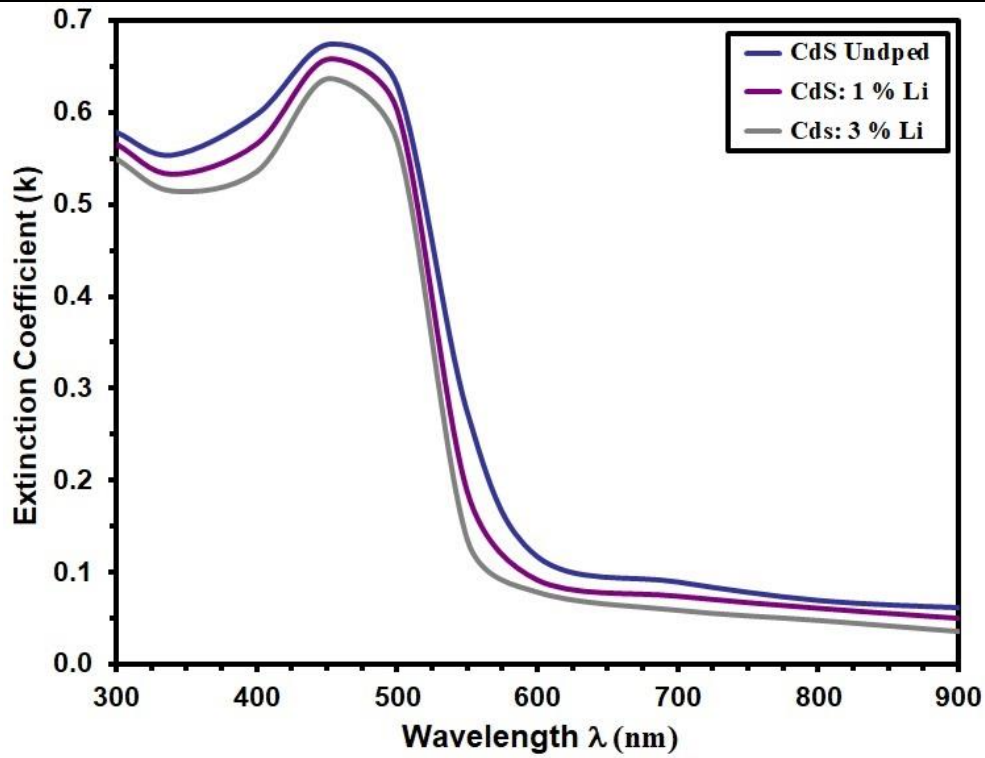


Fig. 7: k_o of the grown films.

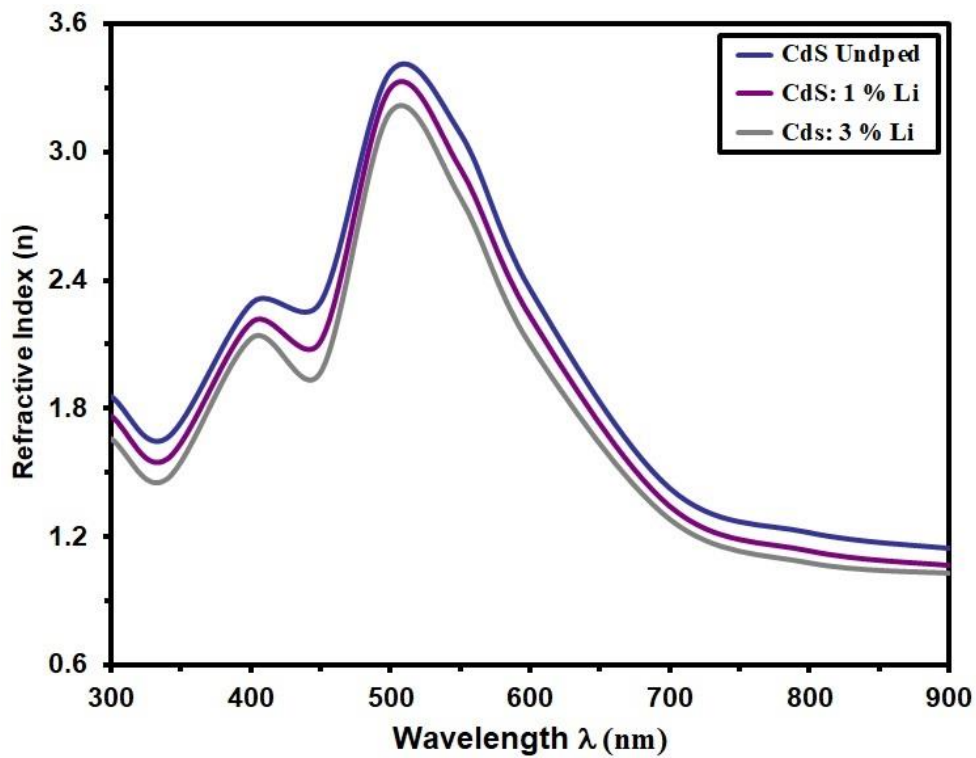


Fig. 8. n of grown films.

Conclusion

Undoped CdS and CdS: Li thin films were fabricated using Spray Pyrolysis Technique at a deposition temperature of 400°C. X-ray diffractogram analysis revealed that the films had a cubic polycrystalline structure with a dominant orientation along the (111) plane. With an elevation in lithium content, there was an observable augmentation in the average grain size of the films, transitioning from 10.11 nm to 11.07 nm. In tandem, the strain (%) parameter underwent a reduction, declining from 34.27 to 31.31. The particle size (T_p) of the deposited films was measured as 87.2 nm for undoped CdS, 75.7 nm for CdS:1% Li, and 33.1 nm for CdS:3% Li, based on AFM images. Furthermore, the average surface roughness (Ra) values decreased from 8.85 nm to 4.34 nm with increasing lithium content, and the RMS values decreased from 9.81 nm to 5.55 nm with doping. The optical bandgap (E_g) decreased with increasing lithium doping, from 2.40 eV to 2.29 eV. Additionally, the UV-Vis transmittance decreased as the lithium content increased, although all films showed transmittance levels greater than 85% for undoped CdS films. Extensive analysis of the effect of lithium doping on some optical characteristics of undoped CdS films revealed that the values of optical constants decreased as the lithium content increased to 3%.

References

- [1] A. Khare, Factors affecting the electro-optical and structural characteristics of nano crystalline Cu doped (Cd-Zn) S films, *J. Phys. Chem. Solids*, 73 (2012) 839–845.
- [2] M. A. Manthrammel, V. Ganesh, S. Mohd, I. S. Yahia, S. AlFalfy, Facile synthesis of Li-doped CdS nanoparticles by microwave assisted co-precipitation technique for optoelectronic application, *Mater. Res. Express*, 6(2018)025022-025029.
- [3] J.S. Jie, W.J. Zhang, Y. Jiang, X.M. Merag, Y.Q. Li, S.T. Lee, Photoconductive characteristics of single-crystal CdS nanoribbons, *Nano Lett.*, 6 (2006) 1887–1892.
- [4] M. Muthusamy, S. Muthukumar, M. Ashokkumar, Composition dependent optical, structural and photoluminescence behaviour of CdS:Al thin films by chemical bath deposition method. *Ceramics International*, 40 (2014) 10657–10666.
- [5] G. Perna, V. Capozzi, M. Ambrico, V. Ligonze, A. Minafra, L.Schiavulli, M. Pallara, Structural and optical characterization of undoped and indium-doped CdS films grown by pulsed laser deposition, *Thin Solid Films*, 453 (2004) 187-194.
- [6] H. Chavez, M. Jordan, J.C. McClure, G. Lush, V.P. Singh, Physical and electrical characterization of CdS films deposited by vacuum evaporation, solution growth and spray pyrolysis, *J. Mater. Sci. Mater. Electron.*, 8 (1997) 151–154.

- [7] F.Lisco, P.M.Kaminski, A.Abbas, K.Bass, J.W.Bowers, G.CiLidio, M.Losurdo, J.M.Walls, The structural properties of CdS deposited by chemical bath deposition and pulsed direct current magnetron sputtering, *Thin Solid Films*, 582(2015)323-327.
- [8] K.K. Challa, E. Magnone, E.-T. Kim, Highly photosensitive properties of CdS thin films doped with boron in high doping levels. *Mater. Lett.*, 85 (2012) 135-137.
- [9] P.K. Singh, P. Kumar, T. Seth, H.-W. Rhee, B. Bhattacharya, Preparation, characterization, and application of Nano CdS doped with alum composite electrolyte. *J. Phys. Chem. Solids*, 73(2012) 1159-1163.
- [10] S. Butt, N.A. Shah, A. Nazir, Z. Ali, A. Maqsood, Influence of film thickness and In-doping on physical properties of CdS thin films. *J. Alloy. Compd.*, 587(2014) 582-587.
- [11] A. Fernández-Pérez, C. Navarrete, P. Valenzuela, W. Gacitúa, E. Mosquera, H. Fernández, Characterization of chemically deposited aluminum-doped CdS thin films with post-deposition thermal annealing. *Thin Solid Films*, 623(2017)127-134.
- [12] E. U. Masumdar, V. B. Gaikwad, V. B. Pujari, P. D. More, L. P. Deshmukh, Some studies on chemically synthesized antimony-doped CdSe thin films, *J. Materials Chemistry and Physics*, 77(2003)669-676.
- [13] R.B. López-Flores, Oscar Portillo Moreno, R. Lozada-Morales, R. Palomino-Merino, The effect of Er³⁺ doping on the physical properties of CdSe thin films deposited by chemical bath, *Revista Mexicana de Fisica*, 52 (2006) 39-41.
- [14] A. M. Perez Gonzalez, I.V. Arreola, C.S. Tepantlán, Effects of indium doping on the structural and optical properties of CdSe thin films deposited by chemical bath, *Revi. Mexican defisica.*,55 (2009)51-54.
- [15] R.R.Pawar, R. A. Bhavsar, S.G. Sonawane, Structural and optical properties of chemical bath deposited Ni doped Cd–Se thin films, *Indian J.Phys.*,86(2012)871-876.
- [16] G. Ojeda-Barrero, A.I. Oliva-Avilés, A.I. Oliva, R.D. Maldonado, M. Acosta, G.M. Alonzo-Medina, Effect of the substrate temperature on the physical properties of sprayed-CdS films by using an Litomatized perfume atomizer. *Mater. Sci. Semicond. Process.*, 79 (2018)7-13.
- [17] S. K. Panda, S. Chakrabarti, A. Ganguly, and S. ChLidhuri, Photoluminescence and Raman Study of CdS–Al₂O₃ Nanocomposite Films Prepared by Sol-Gel Techniques. *Journal of Nanoscience and Nanotechnology*, 5 (2005) 459–465.
- [18] ZiLil Raza Khan, Munirah, Anver Aziz, Mohd. Shahid Khan, Sol-gel derived CdS nanocrystalline thin films: optical and photoconduction properties. *Materials Science-Poland*, 36 (2018) 235-241.
- [19] M. Aslam Manthrammel, Mohd. Shkir, S. Shafik, Mohd. Anis, S. AlFaify, A systematic investigation on physical properties of spray pyrolysis–fabricated CdS thin films for opto-nonlinear applications: An effect of Na doping. *Journal of materials research*, 35 (2020) 410-421.
- [20] I. Mártil de la Plaza, González-Díaz G, Sánchez-Quesada F, Rodríguez-Vidal M. Structural and optical properties of r.f.- sputtered CdS thin films. *Thin Solid Films* 1984;**120**: 31-6.
- [21] Mahdi MA, Kasem SJ, Hassen JJ,Swadi AA,A l-Ani SKJ. Structural and optical properties of chemical deposition CdS thin Films. *Int. J. Nanoelectronics and Materials* 2009; **2**:163-72.
- [22] Ashour A, El-Kadry N, Mahmoud SA. On the electrical and optical properties of CdS films thermally deposited by a modified source. *Thin Solid Films* 1995;**269**:117-20.

[23] DavideBarreca,AlbertoGasparotto,CinziaMaragno, and Eugenio Tondello. CVD of Nanosized ZnS and CdS thin films from

single-source precursors. *J. Electrochem. Soc.* 2004;**151(6)**:G428-35.

[24] Albin D, Rose D, Dhere R, Levi D, Woods L, Swartzlander A, Sheldon P. Processing effects on junction interdiffusion in

CdS/CdTe polycrystalline devices. *Proc. 26th IEEE Photovoltaic Specialists Conf.*, Anaheim, California; 1997.

[25] Humenberger J, Linnert G, Lischka K. Hot-wallepitaxy of CdS thin films and their photoluminescence. *Thin Solid Films* 1984; **121(1)**:75-83.

[26] Haider AJ, Mousa AM, and Al-Jawad SMH. Annealing effect on structural, electrical and optical properties of CdS films prepared by CBD method. *J. Semicond. Technol. Sci.* 2008;**8**:326-332.